Conference on Modelling Fluid Flow (CMFF'22)
The 18th International Conference on Fluid Flow Technologies
Budapest, Hungary, August 30 -September 2, 2022

STUDY ON THE EFFECT OF SUDDEN DUCT DIAMETER CHANGE ON THE PERFORMANCE OF AN AXIAL FLOW FAN

Bálint LENDVAI[1], Tamás BENEDEK[2]

[1] Corresponding Author. Department of Fluid Mechanics, Faculty of Mechanical Engineering, Budapest University of Technology and Economics. Bertalan Lajos u. 4 – 6, H-1111 Budapest, Hungary. Tel.: +36 1 463 2546, E-mail: lendvai.balint@gpk.bme.hu
[2] Department of Fluid Mechanics, Faculty of Mechanical Engineering, Budapest University of Technology and Economics. E-mail: benedek.tamas@gpk.bme.hu

ABSTRACT

The installation of ducted fans has a major impact on their operation. However, axial flow fans are occasionally installed in larger diameter ducts for their small space requirement. This type of installation results in a forward-facing step and a backward-facing step closely upstream and downstream of the fan respectively. These sudden diameter changes cause massive annual separations at the diameter changes, which increases losses in itself, furthermore, the inflow condition is also altered especially close to the tip region of the rotor. The modified inflow condition might result in an increased pressure gradient through the tip gap of the fan, which promotes backflow in the annular region close to the casing. In this paper, we investigate the developed flow field and its effect on the fan performance in the case of an axial flow fan installed in a larger diameter duct at different operating points through computational fluid dynamics simulations.

Keywords: axial flow turbomachinery, backward-facing step, CFD, diameter change, ducted fan, forward-facing step

NOMENCLATURE

c_{mid}	[m]	mid-chord
D	[m]	duct diameter
M	[Nm]	the momentum acting on the rotating surfaces
n	[1/min]	rotation speed
Δp_t	[Pa]	total pressure rise
Q_V	[m^3/s]	flow rate
Re_C	[-]	mid-chordbased Reynolds-number
r_b	[m]	blade tip radius
η	[-]	efficiency
ρ	[kg/ m^3]	density
Φ	[-]	global flow coefficient
φ	[-]	dimensionless axial velocity
φ_c	[-]	dimensionless circumferential velocity
φ_r	[-]	dimensionless radial velocity
Ψ	[-]	total pressure rise coefficient
ψ_t	[-]	dimensionless total pressure

1. INTRODUCTION

Axial flow fans are commonly used in ventilation systems if a relatively high flow rate and low-pressure rise are needed. Based on the application, this type of fan can be installed in various setups, from free-inlet free-exhaust to fully ducted. The inflow conditions of the impeller are heavily impacting the aerodynamic behavior of the fan [1-3]. In the case the inlet velocity profile differs from that prescribed in the design (i.e., free or controlled vortex design [1,4]) or realized during the catalog data measurements, the efficiency may decrease, and the operating point can differ from what was expected.

In the case of free-inlet setup, the inlet flow conditions can be influenced by the intake geometry, for example, bellmouth inlets [5-7]. If the fan is ducted, the developed duct flow determines the inlet velocity profile if the diameter of the duct and the fan casing match. However, in ventilation systems, the diameter of the duct and the fan casing may differ, or the shape of the duct is rectangular instead of a circle. In that case, the inflow conditions are influenced by the flow phenomena induced by the size or shape change. In the case of limited space, the transition between the different sizes or shapes is carried out with sudden changes, which involves the appearance of the boundary layer separation and stagnation zones at the outer radii [8].

Due to the pressure difference between the pressure and suction side of the blade tip, an inevitable tip leakage flow occurs in the gap between the blade tip and the fan casing. The leakage flow is one of the major aerodynamic loss and noise sources of axial flow fans. This leakage flow often rolls up in a tip leakage vortex, which passes through the blade passage in the downstream direction. The strength of

Copyright© Department of Fluid Mechanics, Budapest University of Technology and Economics and the Authors

the leakage flow is affected by the tip gap size, if the gap size is relatively large, the leakage flow becomes more dominant, and the resulted aerodynamic noise and loss (blockage effect of the extended leakage flow and the thickened boundary layer on the annular wall) are increased [9-11]. In case of increased tip gap and decreased axial velocity in the tip region, the exit angle of the leakage vortex measured to the axial direction can be increased, which may result that the leakage vortex impinges on the pressure side of the following blade. In that case, an increased sound emission can be experienced, and the aerodynamic losses are increasing as well as the increased blockage effect of the leakage flow [9, 11]

Based on the above, the disturbed flow at the outer radii caused by the diameter or duct shape change in the vicinity of the fan can amplify the negative effects of the tip leakage flow. In the present paper, the effect of the sudden duct diameter change on the flow behavior of an axial flow is investigated in various operation points using steady-state computational fluid dynamics simulations with special attention to the tip region.

2. SETUP OF CASE STUDY

The investigated low-speed fan (Fig 1.) has 5 forward-skewed controlled vortex design blades with circular arch profiles. The radius of the fan blade tips was $r_b = 0.15\ m$ with a hub-to-tip ratio of 0.3. The fan had no inlet or outlet guide vanes. It was installed in a short duct section (casing) of $0.6\ r_b$ length for all cases. The tip clearance of the fan was set to 5%. The chord length of the blades at mid-span was $c_{mid} = 1.09\ r_b$.

Figure 1: Fan of case study

In the simulations $10\ r_b$ long inlet and outlet ducts were connected to the casing of the fan. This was proved enough for the boundary layer to develop fully. Five inlet and outlet duct diameter were investigated, which was as follows respectively: $D = 315; 400; 500; 630; \infty\ mm$. The duct diameter changes were resolved with forward and backward-facing steps. In the case of the unducted arrangement 1 meter long cylindrical fluid volumes with 1 meter diameter were modeled upstream and downstream of the fan. The schematic drawing is shown in Fig 2.

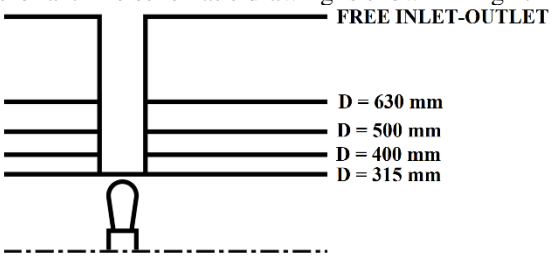

Figure 2: Schematic drawing of the investigated sudden diameter changes

The fan was investigated at $n = 1400\ RPM$ rotational speed. The operation of the fan at different operating points was examined under six flow rates: $\Phi = 0.14; 0.18; 0.22; 0.26; 0.30; 0.34$. Where the flow coefficient was calculated as follows:

$$\Phi = \frac{Q_V}{r_b^3 \cdot \frac{n}{60} \cdot \pi^2 \cdot 2} \tag{2.1}$$

According to the rotational speed and the flow rates, the mid-chord-based Reynolds number of the fan blades varied between $Re_C = 100000 - 110000$.

3. METHODOLOGY

The simulations were carried out in ANSYS Fluent 21R1 software. The Reynolds-averaged Navier Stokes simulations were supplemented with the k-ω shear stress transport turbulence model [12]. The simulation setup is shown in Fig. 3. The axial fan was modeled with the frozen rotor model. The inlet and outlet ducts had a stationary frame of reference. For the ducted arrangements at the duct inlet surface uniform axial velocity profile was prescribed, with velocity magnitude calculated from the flow rate. In order to calculate the turbulence properties at the inlet, turbulence intensity of 5% and the duct hydraulic diameter were set. The outflow was modeled as free exhaust with constant static pressure. Due to the moderate pressure rise and low Mach-number, the fluid was considered incompressible.

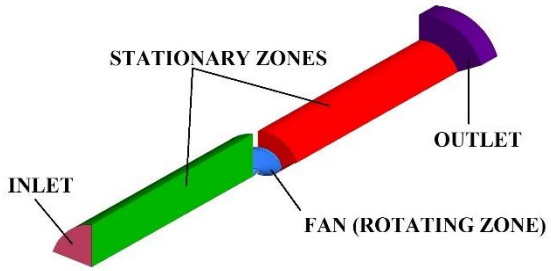

Figure 3: The simulation setup

The numerical meshes (Fig. 4) were constructed utilizing the same rotor mesh and exchanging the different diameter inlet and outlet ducts. The

Copyright© Department of Fluid Mechanics, Budapest University of Technology and Economics and the Authors

structured O-grid mesh of the rotor contained 1.5 million cells, the blade was resolved with 85 by 105 cells in axial and radial directions respectively with more refined mesh near the blade leading edge, trailing edge, blade tip, and near the hub. The tip clearance was divided into 25 cells radially, while the blade tip thickness was modeled with 10 cells. The H-grid duct meshes contained 1.1-2.9 million cells depending on their diameter with high-resolution boundary layer and shear layer meshes. Mesh sensitivity analysis showed the mesh was adequate.

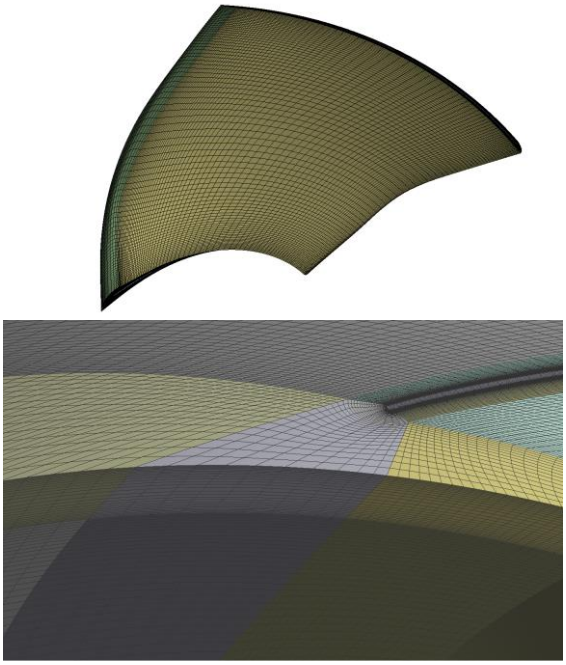

Figure 4: The numerical mesh

From the simulation results, dimensionless characteristic curves (flow coefficient - Φ vs. total pressure rise coefficient - Ψ and flow coefficient – Φ vs. efficiency – η) were derived. The dimensionless quantities were calculated as follows:

$$\Psi = \frac{\Delta p_t}{\rho \cdot r_b^2 \cdot \left(\frac{n}{60}\right)^2 \cdot \pi^2 \cdot 2} \tag{3.1}$$

$$\eta = \frac{Q_V \cdot \Delta p_t}{M \cdot \frac{n}{60} \cdot \pi \cdot 2} \tag{3.2}$$

Besides the characteristic curves, the circumferentially averaged dimensionless velocity (the velocity components are nondimensionalized with the blade tip speed), and total pressure (nondimensionalized with dynamic pressure calculated from the tip speed) profiles in the inlet and outlet cross-section of the casing are also presented, and the typical flow phenomena are visualized.

4. RESULTS

The total pressure rise coefficient and efficiency curves of the fan can be seen in Fig 5. for the investigated duct diameters. It can be concluded that the appropriate diameter ducting clearly outperforms the arrangements with diameter changes in the case of higher flow rates: the total pressure rise and efficiency are lower if the duct size is larger. Furthermore, it can be said in general that the larger the diameter change, the less efficiently the fan operates. It also can be seen the point of maximum efficiency is moving toward the lower flow rates if the duct diameter is increasing. In the case of the lower flow rates, the differences between the curves of different duct diameters are moderate, except for the smallest duct, because the negative effects of the high angle of attack of the blades become more dominant than the losses due to the diameter change.

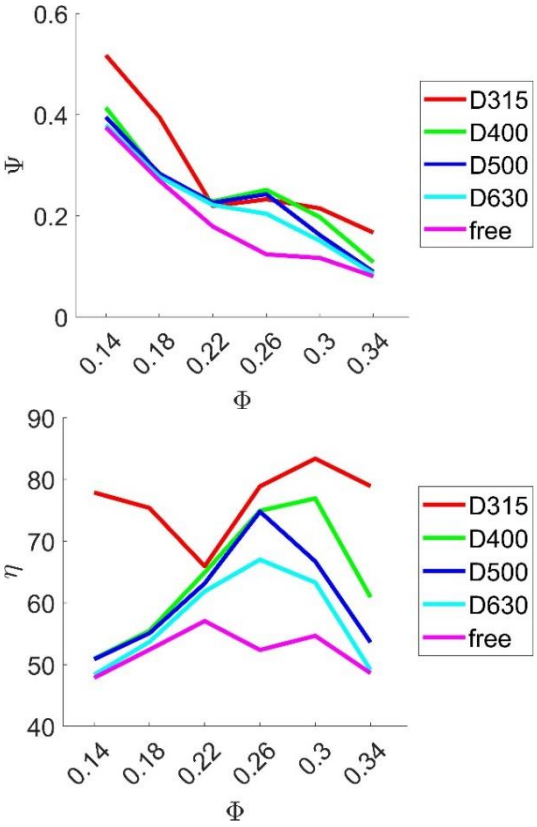

Figure 5: Performance curves

The operation of the fan is also analyzed through pressure and velocity component distributions along the normalized span. The derived curves are shown in Figs. 6-9. for the flow rates of $\Phi = 0.14; 0.22; 0.34$. The distributions of the further investigated flow rates can be found in the appendix. The inlet side distributions are sampled close downstream of the forward-facing step and the outlet side distributions are sampled close upstream of the backward-facing step. This way the immediate effect of the fan blade is reduced. Therefore, a less noisy distribution is obtained. The pressure values were circumferentially averaged based on mass flow rate, and the velocity distributions were area averaged.

Let us investigate the inlet and outlet surfaces separately. The dimensionless axial velocity (φ) profiles are depicted in Fig 6. At the highest

Copyright© Department of Fluid Mechanics, Budapest University of Technology and Economics and the Authors

investigated flow rate the inlet axial velocity, according to the controlled vortex design, constantly increases along the span, until the friction on the duct wall decelerates the flow. In the case of the smallest duct, this decrease in the axial velocity begins at 70% of the span, and in the cases of sudden diameter change, it appears around 95% of the span. The maximum inlet axial velocity moves towards lower radii with the decrease of the flow rate in all of the cases. At the lowest flow rates, a recirculation zone is experienced in the tip region of the inlet, and the backflow intensity increases with the duct diameter increase. In Fig 10. the boundary of the recirculation zones is highlighted for different cases. In this figure, the extension of the recirculation zone with the decrease of the flow rate can be observed in the case of the $400\,mm$ duct diameter. In the case of high flow rate operation, apart from the inevitable separation in the corner of the connection of the duct and the fan casing, backflow does not appear in the inlet duct.

The dimensionless circumferential velocity (φ_c) distributions are shown in Fig 7. In the case of the highest flow rate, the circumferential velocity is nearly zero along the span for all of the ducts. With the decrease of the flow rate, the tangential velocity increases near the casing, and that rotating zone becomes more extensive with the further reduction of the flow rate. This increased circumferential velocity reveals that the backflow originates from the tip region of the blade. In Fig 10. it can be seen in the cases of sudden diameter change, the recirculation zone in the corner of the duct connection and the recirculation from the blade tip interact and form a complex recirculation structure.

The dimensionless radial velocity (φ_r) distributions are depicted in Fig 8. At the highest investigated flow rate, the radial velocity is nearly zero in the case of the smallest duct; however, in the other cases, an intensive downward flow is experienced due to the sudden diameter change. The extension of above mentioned the recirculation zone influence the inlet radial velocity distribution as well: with the appearance of the backflow (i.e., the decrease of the flow rate), the downward flow at the inlet section of the blades becomes more intensive in all of the cases. Besides that, due to the increased tangential and radial velocity, the total pressure also increases near the casing in the inlet section of the impeller, as can be seen in Fig 9.

At the outlet section of the blading, the axial velocity distribution (Fig 6.) is nearly similar in all of the cases at the highest investigated flow rate: the axial velocity is moderate in the boundary layer of the annulus walls and farther from the walls a radially increasing axial velocity can be seen. The maximum axial velocity moves toward the casing wall with the increase of the duct diameter. With the decrease in the flow rate, the boundary layer is thickening on the annulus walls. At the lowest investigated flow rate, if there is no change in the diameter, highly reduced axial velocity is experienced in the wall regions, and the maximum axial velocity can be found around the midspan. In the cases of sudden diameter change, the flow pattern differs from that: in the vicinity of the hub, a recirculation zone forms, which extends until 40% of the span. Due to this recirculation zone, the highest axial velocity values appear in the 70-100% interval of the span. In Fig 10. the formation of more and more dominant hub recirculation zone with the decrease of the flow also can be observed in the case of $400\,mm$ duct diameter. In this figure, the appearance of a recirculation zone at the outlet duct connection corner also can be seen in case of sudden diameter changes. It also can be observed that the size of this corner recirculation zone is increasing with the extension of the hub recirculation zone.

The dimensionless circumferential velocity distribution (Fig 7.) in the outlet section shows a maximum at the border of the hub boundary layer, and moderate values can be seen in the vicinity of the hub at the highest investigated flow rate. Farther from the walls, a slight radial increase is experienced in the case of the smallest duct. The slope of the distribution becomes higher with the increase of the duct diameter. However, the average circumferential velocity decreases with the increase of the duct diameter, which gives an explanation for the poorer performance of the higher diameter setups at the higher flow rates. In the case of the lower flow rates, the circumferential velocity decreases in the forming recirculation zone near the hub if the casing at the duct diameter does not match. From the circumferential velocity distribution, it can also be seen that at the lowest flow rate, the extension of this recirculation zone is extended to 40% of the span. This phenomenon explains the outperformance of the matching duct setup in the cases of lower flow rates. At higher radii, the outlet circumferential velocity increases at moderate flow rates in the low axial velocity zone.

In accordance with the circumferential velocity distribution, at the highest investigated flow rate, outside the annular wall boundary layer, a radially increasing total pressure (Fig 9.) is experienced. If the flow rate is decreased, the total pressure is nearly constant farther from the walls, and at the lowest flow rate significantly decreased total pressure values can be seen in the hub recirculation zone in the cases of sudden diameter change.

In the dimensionless radial velocity distributions (Fig 8.), it can be observed that the radial velocity increases with the increase of the duct diameter due to the displacing effect of the hub recirculation zone. If the flow rate decreases, the maximum values move towards to highest radii, which explains the decreasing size of the corner recirculation zone in the cases of sudden diameter change.

Copyright© Department of Fluid Mechanics, Budapest University of Technology and Economics and the Authors

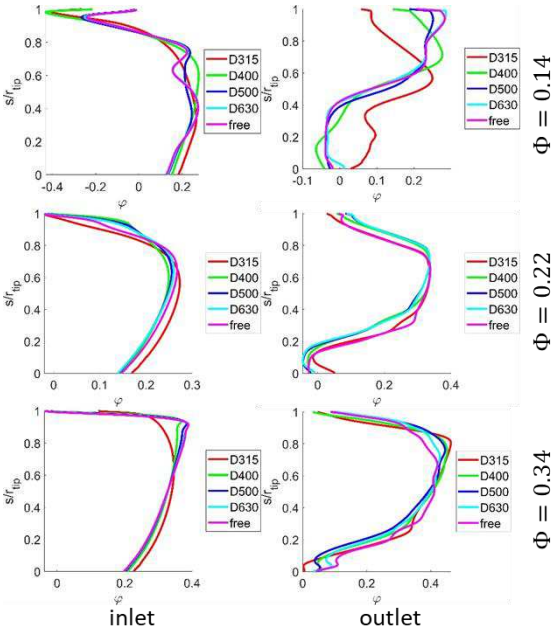

Figure 6: Radial distribution of dimensionless axial velocity at different flow rates close to the forward and backward-facing steps

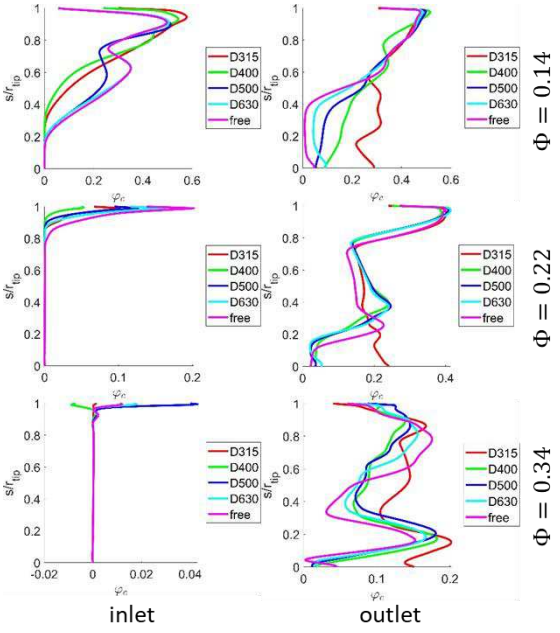

Figure 7: Radial distribution of dimensionless circumferential velocity at different flow rates close to the forward and backward-facing steps

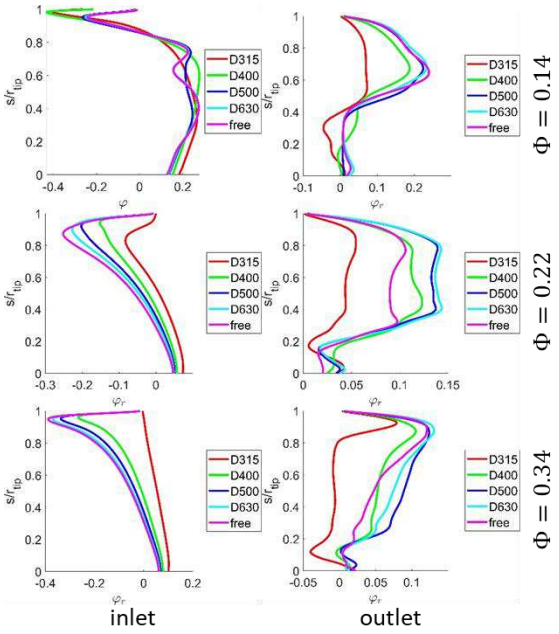

Figure 8: Radial distribution of dimensionless radial velocity at different flow rates close to the forward and backward-facing steps

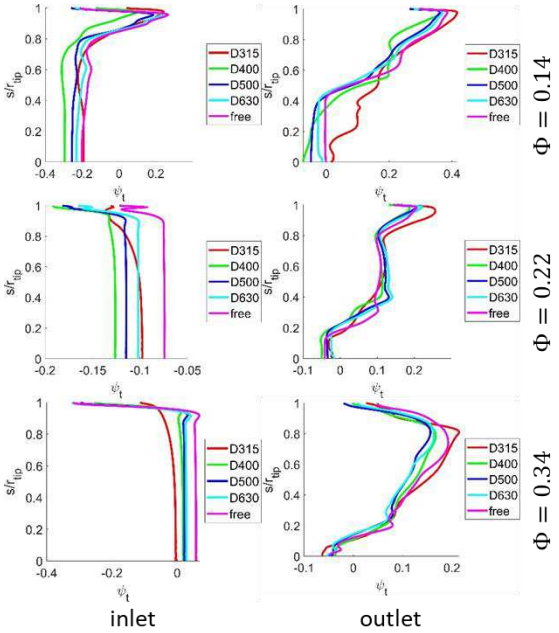

Figure 9: Radial distribution of dimensionless total pressure at different flow rates close to the forward and backward-facing steps

Copyright© Department of Fluid Mechanics, Budapest University of Technology and Economics and the Authors

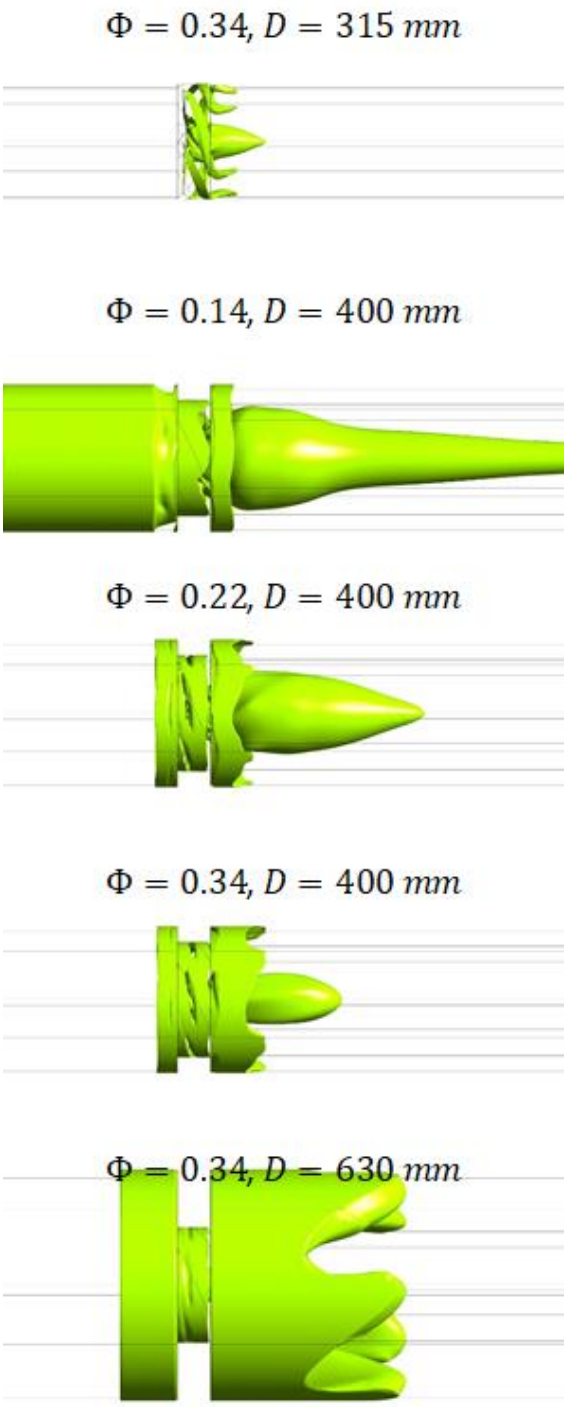

Figure 10. The zero axial velocity iso-surfaces for different duct diameters and operating points

5. SUMMARY

In the present paper, the effect of the sudden diameter changes on the performance of an axial flow fan was investigated using computational fluid mechanics simulations. The fan was placed in a short casing with a diameter of $315\ mm$. The diameter of the connecting ducts varied between $315 - \infty\ mm$. The fan was investigated at constant rotational speed in the $\Phi = 0.14 - 0.34$ flow rate interval. The mid-chord-based Reynolds number of the blades varied between $Re_C = 100000 - 110000$.

In accordance with the expectations, the calculated total pressure rise and efficiency curves showed that the setup without sudden diameter changes outperforms the other cases in the investigated flow rate interval. At the higher investigated flow rates, the total pressure rise, and the efficiency decreased with the increase of the connecting duct diameter. At the lower investigated flow rates, there was no significant difference between the curves of different duct diameters.

The circumferentially averaged velocity and total pressure profiles in the inlet and outlet surface of the blading were also investigated. Based on these profiles and flow visualization, four recirculation zones were found in the cases of sudden diameter changes (see Fig 11): two in the corners of the duct connections, one in the tip region, and one in the vicinity of the hub. The simulation showed that the blade tip recirculation zone becomes more dominant and interacts with the inlet corner recirculation zone with the decrease of the flow rate. In the outlet section, the hub recirculation zone expanded to 40% span at lower flow rates in the cases of sudden diameter changes. In this recirculation zone, the tangential velocity and the total pressure were moderate. The hub recirculation zone was less dominant in the case of the matching duct diameter which explains the outperformance of this setup in the lower flow rate interval. The results also showed that due to the displacing effect of the hub recirculation zone a significant outward flow forms in the cases of sudden diameter change, which cause the contraction of the corner recirculation zone in the outlet duct.

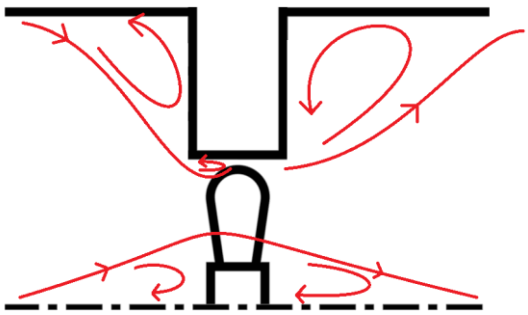

Figure 11: The structure of the separation zones

ACKNOWLEDGEMENTS

This work has been supported by the Hungarian National Research, Development, and Innovation Fund under contract NKFI K 129023.

Copyright© Department of Fluid Mechanics, Budapest University of Technology and Economics and the Authors

APPENDIX

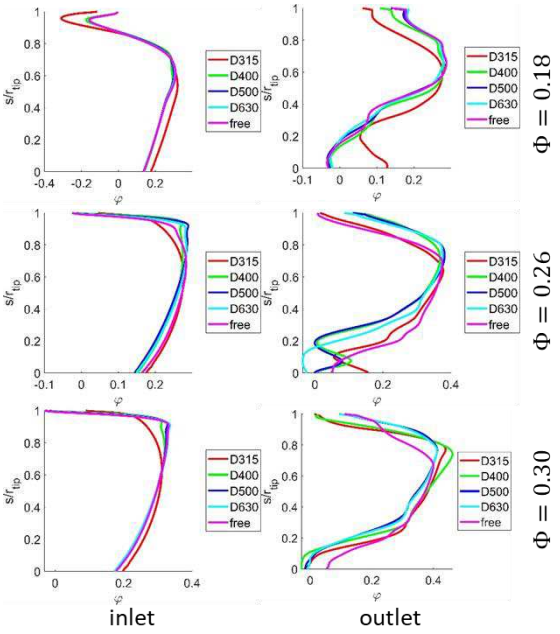

Figure 12: Radial distribution of dimensionless axial velocity at different flow rates close to the forward and backward-facing steps

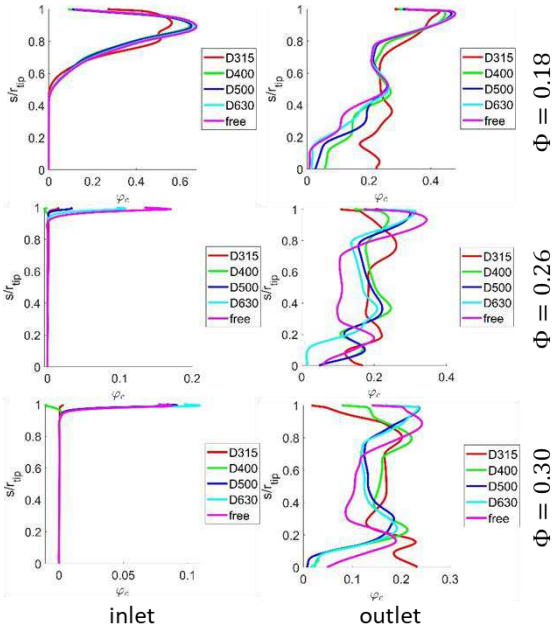

Figure 13: Radial distribution of dimensionless circumferential velocity at different flow rates close to the forward and backward-facing steps

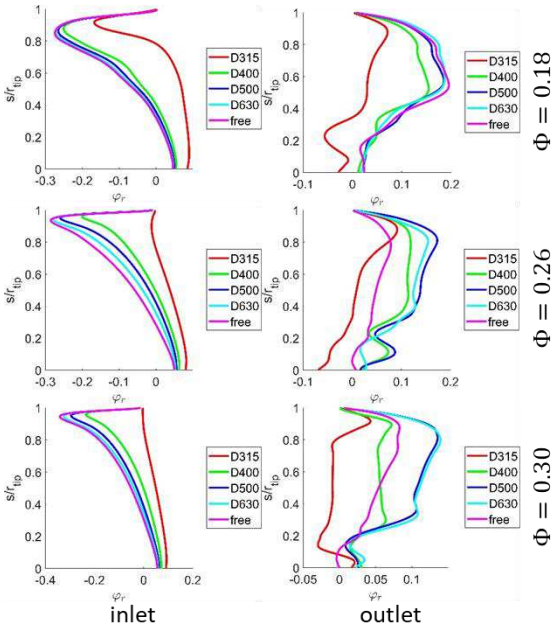

Figure 14: Radial distribution of dimensionless radial velocity at different flow rates close to the forward and backward-facing steps

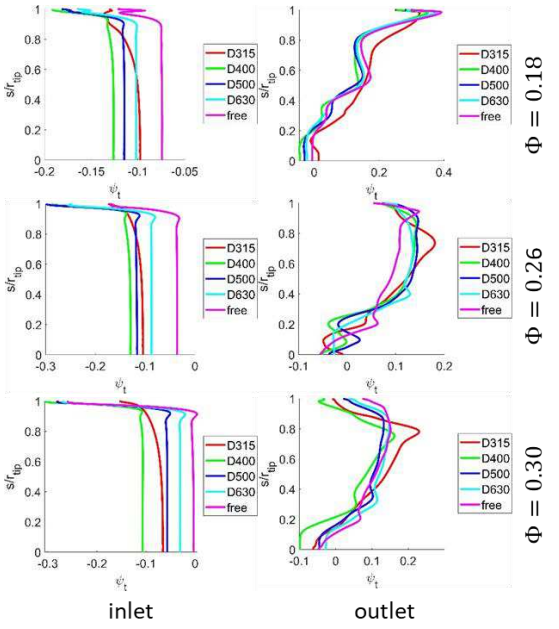

Figure 15: Radial distribution of dimensionless total pressure at different flow rates close to the forward and backward-facing steps

REFERENCES

[1] Carolus, T., 2003, *Ventilatoren* [Fans], 3rd Edition, Teubner Verlag, Germany

[2] Wallis, R. A., 1961, *Axial Flow Fans: Design and Practice*, George Newnes Limited, London, UK

Copyright© Department of Fluid Mechanics, Budapest University of Technology and Economics and the Authors

[3] Daly, B. B., 1992, *Woods Practical Guide to Fan Engineering* (sixth impression), Woods of Colchester Ltd., UK

[4] Vad, J., 2013, "Forward blade sweep applied to low-speed axial fan rotors of controlled vortex design: an overview", *Journal of Engineering for Gas Turbines and Power Transactions of the ASME,* Vol. 135(1), Paper: 012601

[5] Benedek, T., Vad, J., and Lendvai, B., 2022, "Combined acoustic and aerodynamic investigation of the effect of inlet geometry on tip leakage flow noise of free-inlet free-exhaust low-speed axial flow fans", *Applied Acoustics* Vol. 187, Paper: 108488

[6] EN ISO 5801:2018 - Fans - Performance testing using standardized airways (ISO 5801:2017), Standard, International Organization for Standardization, Geneva, CH

[7] Stütz, W., 1996, „Untersuchungen zu der wechselwirkung zwischen einlaufduese und axialventilator" [investigations on the interaction between entry geometry and axial fan], *Tech. Rep*. VDI Berichte Nr. 1249, Verein Deutscher Ingenieure

[8] Lukács, E., and Vad, J., 2021, "Flow topology and loss analysis of a square-to-square sudden expansion relevant to HVAC systems: A case study", *Journal of Building Engineering,* Vol. 41, Paper: 102802

[9] Fukano, T., and Jang, C.-M., 2004, "Tip clearance noise of axial flow fans operating at design and off-design condition", *Journal of Sound and Vibration,* Vol. 275(3), pp. 1027-1050.

[10] Hah, C., 2017, Effects of double-leakage tip clearance flow on the performance of a compressor stage with a large rotor tip gap, *Journal of Turbomachinery Transactions of the ASME,* Vol. 139, Paper: 061006.

[11] Mao, X., Liu, B., and Zhao, H., 2019, "Effects of tip clearance size on the unsteady flow behaviors and performance in a counter-rotating axial flow compressor", *Proceedings of the Institution of Mechanical Engineers, Part G: Journal of Aerospace Engineering,* Vol. 233(3), pp. 1059-1070.

[12] Menter, F. R., 1993, "Zonal Two Equation k-ω Turbulence Models For Aerodynamic Flows", *23rd Fluid Dynamics, Plasmadynamics, and Laser Conference*

Copyright© Department of Fluid Mechanics, Budapest University of Technology and Economics and the Authors